Supplementary Information

Highly Dispersible, Superparamagnetic Magnetite Nanoflowers for Magnetic Resonance Imaging

Fengqin Hu, Keith W. MacRenaris, Emily A. Waters, Elise A. Schultz-Sikma, Amanda L. Eckermann and Thomas J. Meade*

Department of Chemistry, Biochemistry and Molecular Biology and Cell Biology, Neurobiology and Physiology, and Radiology, Northwestern University, Evanston, IL 60208 (USA). E-mail: tmeade@northwestern.edu; Fax: +1 847 491 3832; Tel: +1 847 491 2481

Experiments

Synthesis of the Fe_3O_4 nanoflowers: The synthesis of 30±5 nm Fe_3O_4 nanoflowers (NFs) is as follows: Iron (III) acetylacetonate ($Fe(acac)_3$, 1.5 mmol, 99.9+%, Aldrich), poly(ethylene glycol) bis(carboxymethyl) ether (HOOC-PEG-COOH, 6 g, Aldrich, 600 g/mol), oleylamine (1.93 mL, 70%, Aldrich) and phenyl ether (25 mL, 99%, Aldrich) were mixed and purged with nitrogen. The reaction mixture was heated to 260°C for 24 h, producing a black, homogeneous, colloidal suspension. After cooling to room temperature, 250 mL petroleum ether/ether (v:v=3:1) was added to the reaction solution and resulted in a black precipitate of magnetite NFs that were separated by centrifugation. After washing with petroleum ether/ether (v:v=3:1) three times, the precipitate was re-dispersed in water. The obtained aqueous solution was dialyzed against water for two days and then centrifuged at 4000 rpm for 20 min. After removing the precipitate, the Fe_3O_4 NFs in the supernatant were precipitated by centrifugation at 13,200 rpm for 30 min. After washing with water three times, the Fe_3O_4 NFs were re-dispersed in water. 42±8 nm and 19±3 nm Fe_3O_4 NFs were prepared by decreasing the quantity of HOOC-PEG-COOH (3 g for 42 nm Fe_3O_4 NFs, 4.5 g for 19 nm Fe_3O_4 NFs) and oleylamine (0.96 mL for 42 nm Fe_3O_4 NFs, 1.44 mL for 19 nm Fe_3O_4 NFs) and using shorter reaction times at 260°C (3 h for 42 nm Fe_3O_4 NFs, 20 h for 19 nm Fe_3O_4 NFs). Post-synthesis processing procedures were the same as described in the synthesis of 30 nm Fe_3O_4 NFs.

Cell culture: NIH/3T3 cells were grown in DMEM supplemented with 10% CBS. All cells were grown in a humidified incubator at 37°C and 5% CO_2. All flasks and multi-well plates were tissue culture treated and sterile. NIH/3T3 cells were grown in 24-well tissue-culture plates to approximately 70% confluence prior to experiments.

Cell viability experiments: Fe_3O_4 NFs (in PBS) were diluted in cell media and vortexed. NIH/3T3 cells were incubated with Fe_3O_4 NFs at 37°C and 5% CO_2 for 24 h followed by two rinses with 0.5 mL of DPBS. Cells were detached using a 0.25% trypsin/EDTA solution. Cells were counted and percent viability determined using a Guava Easycyte Mini personal cell analyzer (Guava Technologies, Hayward, CA). Specifically, 20 μL cell samples were diluted 10-fold with Guava ViaCount reagent (total volume of 200 μL). Cells were allowed to stain at room temperature for 5-20 minutes. Samples were vortexed and analyzed using the Guava ViaCount software module (1000 trials per run).

Characterization

TEM images and selected area electron diffraction patterns were obtained on a Hitachi H-8100 operated at an accelerating voltage of 200 kV. High resolution TEM images were obtained on a JEOL JEM-2100F FAST TEM operated at an accelerating voltage of 200 kV. Samples for TEM and high

resolution TEM analysis were prepared by spreading a drop of the solution sample on copper grids coated with a carbon film followed by evaporation under ambient conditions. XRD measurements were performed on a powder sample of the Fe_3O_4 NFs using a Scintag XDS2000 goniometer. DLS measurements were performed with a Malvern Instruments Zetasizer Nano Series Nano-ZS with Dispersion Technology Software 5.03 (Worcestershire, United Kingdom). FTIR spectra were obtained on a Thermo Nicolet NEXUS 870 Fourier transform spectrometer (Thermo Scientific, Waltham, MA). Magnetic susceptibility measurements were carried out on a Quantum Design MPMS5 SQUID magnetometer (San Diego, CA). Samples were dispersed in water and frozen under a nitrogen environment.

MR phantom images were collected at 4.7 T (~ 200 MHz) and ambient temperature (~ 25°C) on a 4.7 T horizontal-bore Bruker Biospec MR imager (Billerica, MA). A T_2-weighted image was acquired using a multi-slice multi echo pulse sequence (TR = 2000 ms, TE = 10 ms, 16 echoes). Images were acquired with field of view (FOV) = 3 × 3 cm^2, data matrix = 256 × 256, slice thickness = 1.5 mm, and 2 signal averages. T_2 was measured with a static TR (2000 ms) and variable TE (10, 40, 80, 160, 400 ms) values. Transverse relaxation times were also measured at 1.5 T (60 MHz) and 37°C on a Bruker mq60 NMR Analyzer equipped with the Minispec V2.51 Rev.00/NT software (Billerica, MA). A spin-echo pulse sequence was used to measure transverse relaxation times. The iron concentration of each sample for SQUID, MRI and relaxivity was determined by Inductively Coupled Plasma Atomic Emission Spectroscopy (ICP-AES, Varian).

Investigation on the reasons for the formation of Fe_3O_4 NFs instead of individual nanoparticles

There are two possible mechanisms for the formation of the Fe_3O_4 nanoclusters. One is that HOOC-PEG-COOH acts as a linker between Fe_3O_4 nanoparticles; the other is that the Fe_3O_4 nanoparticles spontaneously aggregate to form three-dimensional clusters. For this synthesis process, when HOOC-PEG-COOH (600 g/mol) was replaced by HOOC-PEG-COOH (2000 g/mol), 8 nm Fe_3O_4 nanoparticles instead of nanoclusters were obtained.[1] This result indicates that HOOC-PEG-COOH molecules do not act as linkers between nanoparticles. Furthermore, our investigation on the nanostructure morphology at various reaction times showed that there was no individual nanoparticle stage during the reaction period, i. e., the formation of the Fe_3O_4 nanoparticles and the clustering of these nanoparticles are simultaneous (Fig. S1). According to these results, we hypothesize that the Fe_3O_4 nanoparticles spontaneously aggregate to form flowerlike three-dimensional clusters due to their high surface energy in this reaction system.

Fig. S1. TEM images of the nanostructures at various reaction times: a) 10 h; (b) 16 h; (c) 24 h.

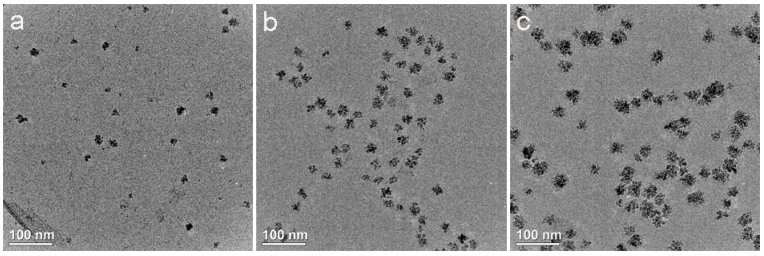

Fig. S2. TEM images of the Fe_3O_4 nanostructures prepared (a) with or (b) without oleylamine.

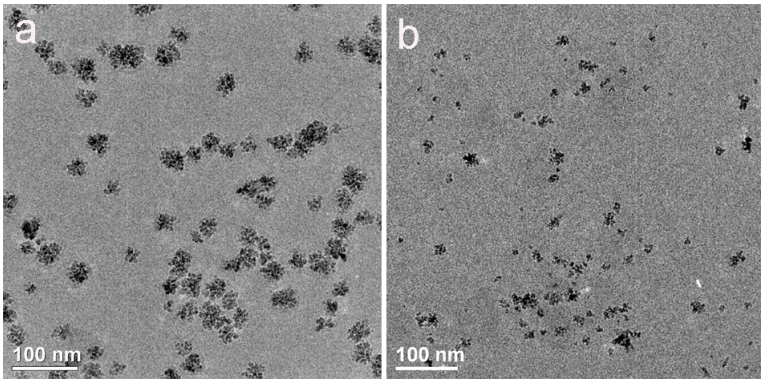

Fig. S3. High resolution TEM images of (a) 42 nm and (b) 19 nm Fe_3O_4 NFs. Scale bar: 10 nm.

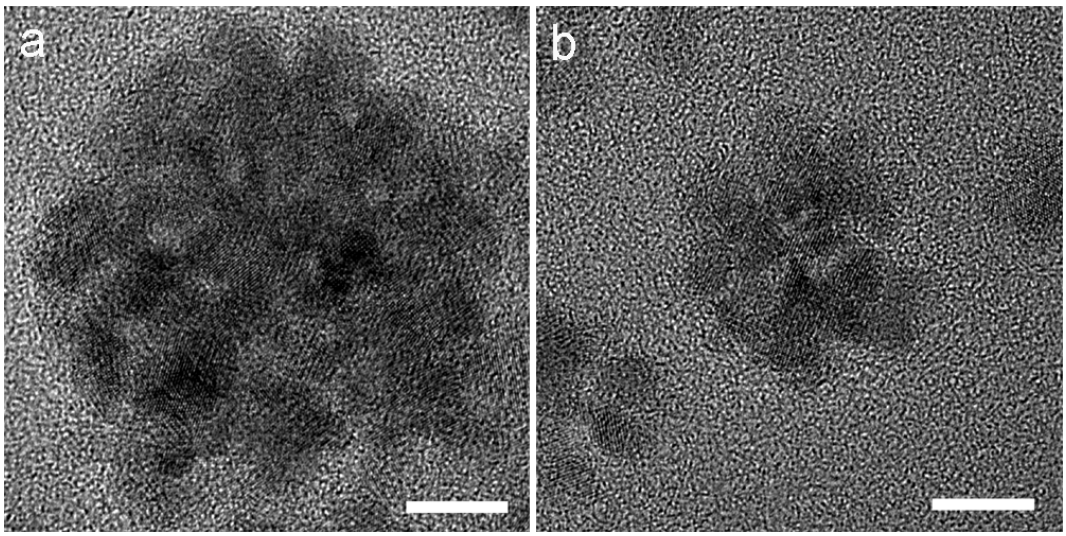

Fig. S4. Powder X-ray diffractograms of (a) 42 nm, (b) 30 nm and (c) 19 nm Fe_3O_4 NFs. Bars: JCPDS card (19-0629) data for magnetite.

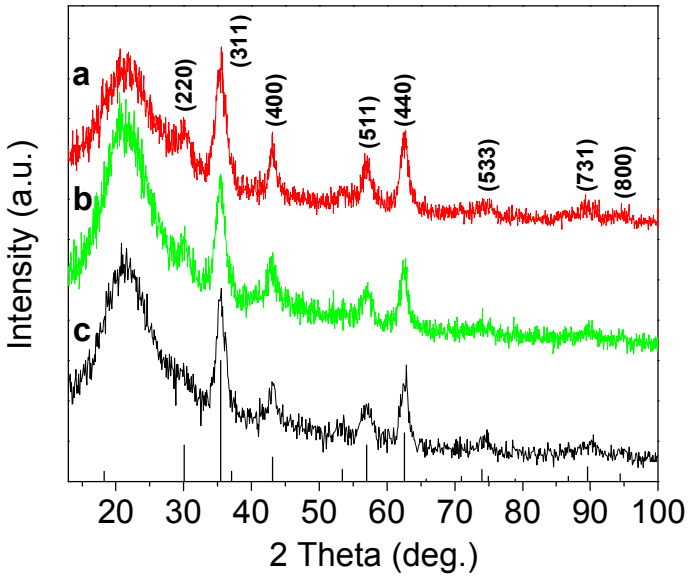

Fig. S5. FTIR spectra of (a) 42 nm, (b) 30 nm and (c) 19 nm Fe_3O_4 NFs. Spectrum d was recorded from the parent HOOC-PEG-COOH.

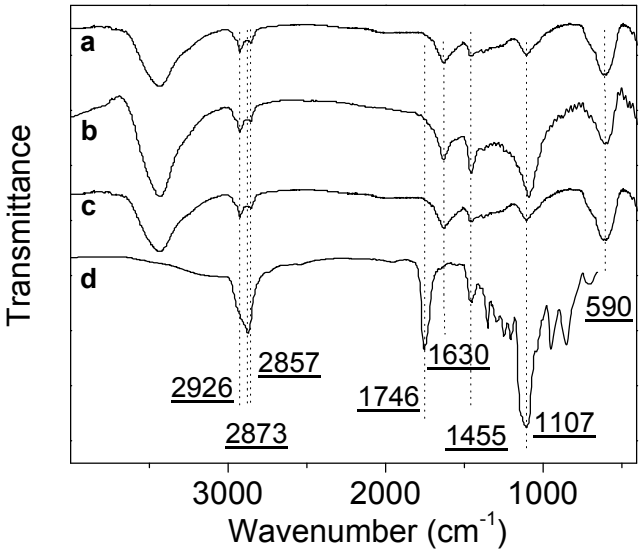

Fig. S6. Hydrodynamic size distributions of 42 nm, 30 nm and 19 nm Fe_3O_4 NFs.

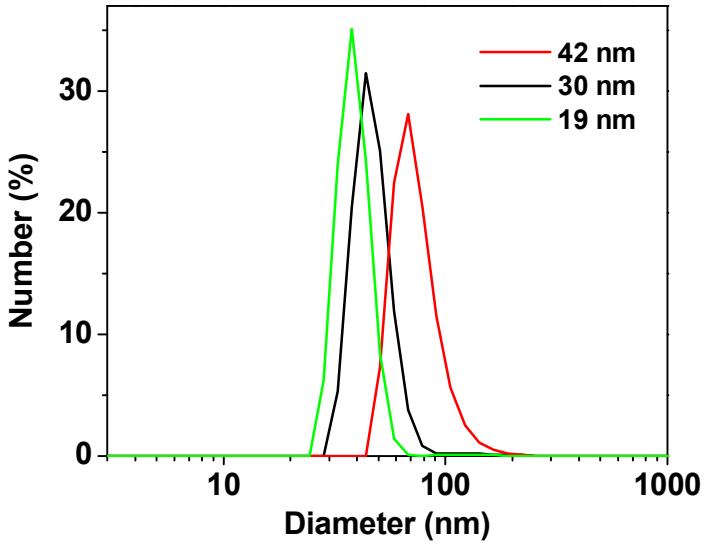

Fig. S7. The hydrodynamic sizes of 30 nm Fe_3O_4 NFs at 0 day and after placement for 21 days under various conditions: (1) H_2O, pH 3; (2) H_2O, pH 5; (3) H_2O, pH 7; (4) H_2O, pH 9; (5) H_2O, pH 11; (6) PBS; (7) 0 M NaCl; (8) 0.25 M NaCl; (9) 0.50 M NaCl; (10) 1.00 M NaCl; (11) DMEM; (12) EMEM.

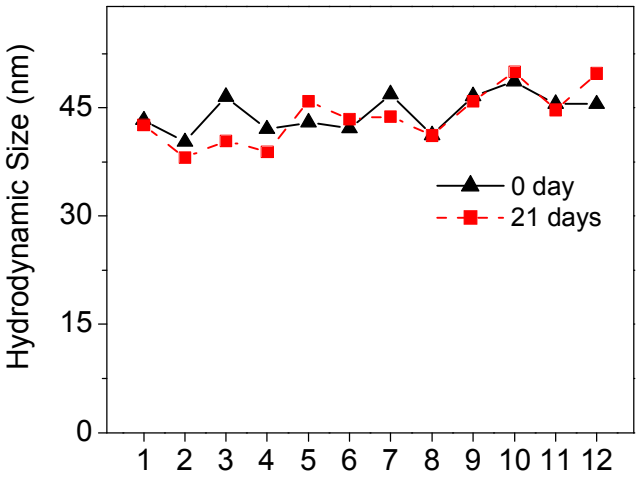

Fig. S8. Temporal evolutions of transverse relaxation time (T_2) of 30 nm Fe_3O_4 NFs in PBS, FBS, CBS, DMEM supplemented with 10% CBS, DMEM supplemented with 10% FBS and EMEM supplemented with 10% FBS (Fe concentration: 22 mg/L). A Carr-Purcell-Meiboom-Gill (CPMG) pulse sequence was used to measure T_2.

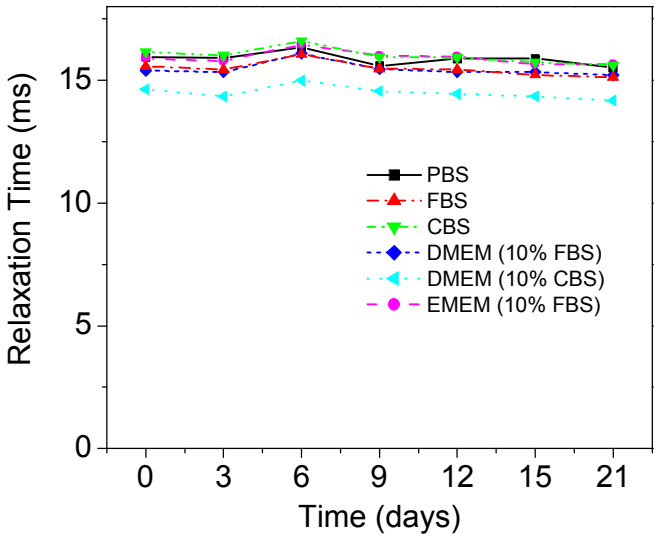

Fig. S9. Zeta potentials of 30 nm Fe_3O_4 NFs under different pH conditions.

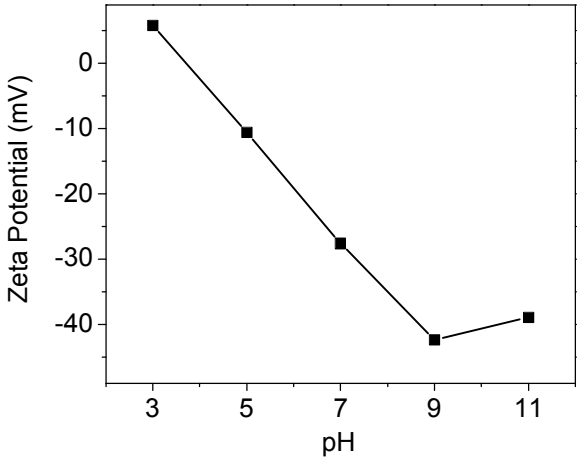

Fig. S10. T_2 relaxation rates ($1/T_2$) plotted against the Fe concentrations of 42 nm, 30 nm and 19 nm Fe_3O_4 NFs (1.5 T, 37°C).

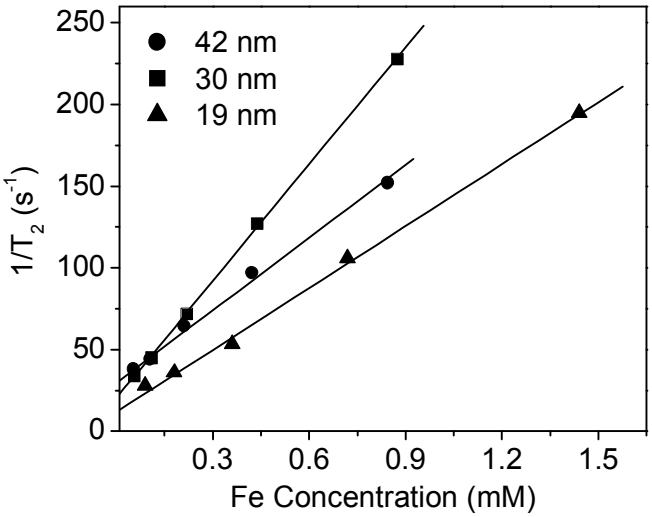

Investigation on the r_2 differences between 30 nm, 42 nm and 19 nm Fe_3O_4 NFs

The MR contrast effect of magnetic agglomerates is expressed as

$$\frac{1}{T_2} = \left(\frac{64\pi}{135}\right)\left(\mu N_g \frac{L(x)}{4\pi}\right)^2 \frac{N_A C_a}{R_a D}$$

where μ = magnetic moment of the nanoparticle, N_g = number of nanoparticles in an agglomerate, $L(x)$ = Langevin function, N_A = Avogadro's number, C_a = concentration of agglomerates, R_a = radius of an agglomerate, and D = water diffusion coefficient.[2,3] According to this equation, $1/T_2$ is proportional to μ and N_g. Based on the primary nanoparticle sizes of the NFs (4.3 nm for 42 nm Fe_3O_4 NFs, 4.8 nm for 30 nm Fe_3O_4 NFs, and 4.5 nm for 19 nm Fe_3O_4 NFs) (Table S1), μ(30 nm NFs) > μ(19 nm NFs) > μ(42 nm NFs). Another parameter, N_g, can be determined by the overall size of the NFs and their primary nanoparticle size. Calculation results demonstrated that N_g(42 nm NFs) > N_g(30 nm NFs) > N_g(19 nm NFs). The synergistic effects of μ and N_g produce the experimental results, r_2(30 nm NFs) > r_2(42 nm NFs) > r_2(19 nm NFs).

Table S1. TEM size, primary Fe_3O_4 nanoparticle (NP) size, hydrodynamic size (D_H), zeta potential, saturation magnetization (M_S) at 250 K, transverse relaxivity (r_2) at 1.5 T and 4.7 T of 30 nm, 42 nm and 19 nm Fe_3O_4 NFs.

TEM size (nm)	Fe_3O_4 NP size (nm)	D_H (nm)	zeta potential (mV)	M_S (emu/g Fe)	r_2 at 1.5 T (mM^{-1} s^{-1})	r_2 at 4.7 T (mM^{-1} s^{-1})
30±5	4.8	47±9	-28	45	238	193
42±8	4.3	74±19	-26	33	148	97
19±3	4.5	39±6	-12	36	126	88

1 S. Liu, B. Jia, R. Qiao, Z. Yang, Z. Yu, Z. Liu, K. Liu, J. Shi, H. Ouyang, F. Wang, and M. Gao, *Mol. Pharmaceutics*, 2009, **6**, 1074.

2 J. Cheon, and J. H. Lee, *Acc. Chem. Res.*, 2008, **41**, 1630.

3 S. Laurent, D. Forge, M. Port, A. Roch, C. Robic, L. V. Elst, and R. N. Muller, *Chem. Rev.*, 2008, **108**, 2064.